

# Research on Automatic Highway Extraction Technology Based on Spectral Information of Remote Sensing Images

Qing-Zhou Ye<sup>1,3,\*</sup>, Ping Wu<sup>2</sup>, Mao-Lin Zhang<sup>1,3,\*\*</sup>

<sup>1</sup>School of Information Science and Engineering  
FuJian University of Technology  
No3 Xueyuan Road, University Town, Minhou, Fuzhou City, Fujian Province, China  
\*yeqz202@126.com; \*\*mailzml@163.com

<sup>2</sup>Fujian Provincial Geomatics Center  
No205 HuaLin Road, Fuzhou City, Fujian Province, China  
76991857@qq.com

<sup>3</sup>Fujian Provincial Key Laboratory of Digital Equipment  
FuJian University of Technology  
No3 Xueyuan Road, University Town, Minhou, Fuzhou City, Fujian Province, China  
\*yeqz202@126.com; \*\*mailzml@163.com

Received March, 2016; revised December, 2016

---

**ABSTRACT.** *In order to solve the problem that the framework of highway cannot be extracted automatically from a static picture, in this paper, an automatic extraction technology is proposed, which is a mathematical morphology method based on the spectral information of the Remote Sensing Image to achieve the automatic highway extraction. The experimental results show that our proposal is effective.*

**Keywords:** Spectral information, Mathematical morphology method, Highway, Automatic extraction

---

1. **Introduction.** Nowadays, among the road extraction, the highway extraction occupies the considerable proportion. However, currently, major highway extraction approaches are still manual. As the manual methods are laborious and time-consuming, with the rapid development of the highway network in China, the automatic extraction of roads becomes very urgent. In the explorations of automatic extraction of the highway, a lot of the relevant algorithms and models have been developed by domestic and foreign scholars[1-4]. However, these algorithms and models are only suitable for some specific fields and the remote sensing images have not been utilized yet. In this paper, we propose an automatic highway extraction technology, which is a technology derived from the characteristic analysis of spectral information of remote sensing images.

2. **Features of image data and ground objects.** Currently, the image sources of the factors collection are mostly from the domestic satellites with the moderate resolution, which are ZY-3, GF-1, TH-1 and so on. These satellite images commonly have the feature of multi-spectral bands, which are blue, green, red, near infrared, and panchromatic. The multi-spectral bands parameters and the resolution of the three satellites are similar too.

Thus, the characteristics of two similar ground objects in these satellite images are also similar, which means that the similar ground objects can be handled by the same methods.

There are several characteristics of the highways in these images. Firstly, the color of the highway itself presents a uniform dark shade in the combination of true color bands, but the distinction between the highway and background is not apparent. Secondly, the larger vehicles on the highways are presented as point targets, but the smaller ones cannot be recognized. Thirdly, there are buildings around the highways, which in general are combined with the road into one. Lastly, the shadows of the highways are so remarkable that they cannot be easily separated from the road. For these reasons, it is difficult to use a single method to extract the highways from the images. To this end, an automatic highway extraction technology based on spectral information is proposed, which will be discussed in details in the next section.

### 3. Automatic highway extraction technology based on spectral information.

The basic working principles of our proposal are: firstly, the transformations of the color space are calculated by combining different bands of remote sensing images, which may distinguish the artificial ground objects from the images with different spectral information; then, the highway centerlines will be further extracted from the highway body by separating the highways and the surroundings through the mathematical morphology of images[5]. In Figure 1, the technological roadmap of the strategies is shown.

**3.1. Remote sensing image preprocessing.** The preprocessing of remote sensing images, including the correction and fusion of panchromatic and multispectral images, which is conducted to enhance image features and improve the interpretation of images. There is using quadratic polynomial for correcting processing, the calculate formula is as follows:

$$\begin{cases} x = a_0 + a_1 \times X + a_2 \times Y + a_3 \times X^2 + a_4 \times X \times Y + a_5 \times Y^2 \\ y = b_0 + b_1 \times X + b_2 \times Y + b_3 \times X^2 + b_4 \times X \times Y + b_5 \times Y^2 \end{cases} \quad (1)$$

In the calculate formula, (x,y) is image ranks value, (X,Y) is ground coordinates  $a_0, a_1, a_2, a_3, a_4, a_5, b_0, b_1, b_2, b_3, b_4, b_5$  are quadratic polynomial coefficients. Fusion processing formula is as follows:

$$\begin{cases} F(n_1, n_2) = C_1 A(n_1, n_2) + C_2 B(n_1, n_2) \end{cases} \quad (2)$$

Wherein,  $n_1$  is the pixels line number of image,  $n_2$  is the pixels row number of image,  $A(n_1, n_2)$  is the pixel of image A,  $B(n_1, n_2)$  is the pixel of image B,  $C_1, C_2$  are weighting coefficients. Figure 2 shows two preprocessing images of ZY-3 satellite used in the experiments, and the original bands of which are blue, green, red and near-infrared. These two images are represented in the true color, i.e. a combination of the red, green and blue bands.

**3.2. Artificial ground objects extracted by spectral information.** As the multi-spectrum remote sensing images have more spectral bands than the conventional ones, they may provide more information of remote sensing and contribute to a more precise classification of the features. Tong Qing-xi et al. classified the reflectance spectral characteristics of different ground objects and indicated the characteristics of artificial ground objects, water and vegetation vary considerably. Thus, the spectral curves can be used to distinguish the artificial ground objects from the other ones[6-7].

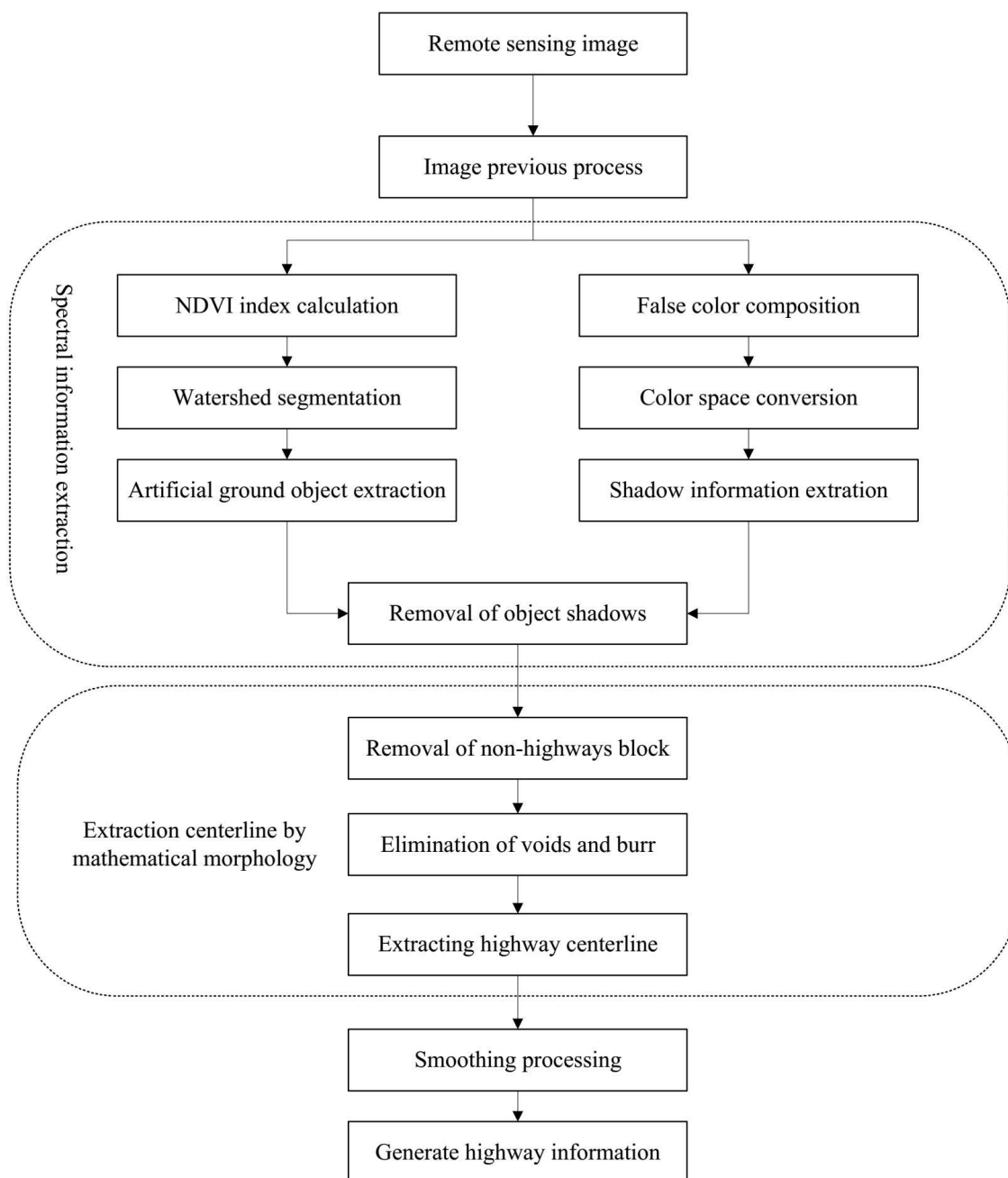


FIGURE 1. The technical roadmap

3.2.1. *Artificial ground objects extraction by using vegetation index information.* The characteristics of the leaf involve the strong absorption in the red band and the reflection in the near infrared band. The vegetation indices may be obtained by combining these two bands. The general vegetation in these vegetation indices is the normalized difference vegetation index (NDVI), which is used to detect the state of vegetation growth, vegetation coverage and eliminate radiation error, etc. The calculation formula is as follows:

$$NDVI = \frac{NIR - R}{NIR + R} \quad (3)$$



FIGURE 2. Experimental images

where NIR is the near infrared band and R is the red band. NDVI value ranges from -1 to 1, where the negative values indicate that the ground is covered by cloud, water, snow, etc., which have the high reflectance of visible light; 0 means that there is a rock or bare soil, etc., and the values of near infrared and red band are approximately equal; the positive values, which increase with the increasing of vegetation coverage, mean that the vegetation covers the ground. The NDVI values of images in Figure 2 are shown in Figure 3, which are normalized with the original NDVI.



FIGURE 3. NDVI index images

As can be seen in Figure 3, the colors of objects like buildings, highways and artificial ground objects in the NDVI index images are shown as dark shade, and the color of the vegetation is shown as bright. The image contrasts of them are very distinguishable. Thus, the artificial ground objects may be identified from the vegetation with reasonable segmentation.

Watershed segmentation algorithm is a kind of segmentation method based on topological theory[8]. The basic idea of it is to take the image as a landscape of geography, in which the gray value of each pixel indicates the altitude and each local minimum and the relevant area are called the reception basin. Through determining the position of the watershed, which is the boundary of the reception basin, the images can be divided into different regions with a group of closed curves. The statistical and experimental NDVI of the images by using watershed algorithm shows that when the segmentation threshold is -0.46, the artificial objects may be effectively separated from the vegetation area and have few incorrect segmentation. Figure 4 shows the mask images of the artificial ground objects extracted by using the watershed algorithm, and its obvious that the main body

of the artificial objects has been stripped mostly from the background images. However, these extraction images have some flaws, i.e. the shadows around the highways cannot be distinguished, which can be seen in Figure 5. Thus, the next step is to separate shadow from artificial ground objects.

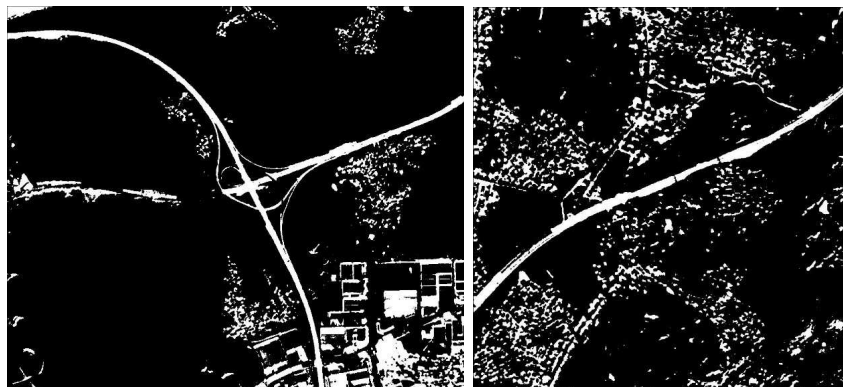


FIGURE 4. The artificial ground objects mask images



FIGURE 5. The shadow that is not removed in the mask image

3.2.2. *Using HSI space to remove the object shadow.* As shown in Figure 2, the distinctions between the artificial ground objects and the background ones are not remarkable. In order to increase the distinctions, the color of the original images is transformed as the false one, whose alternative bands are given in Table 1.

TABLE 1. The band combination used by the false color synthetic image

Original image band	Red band	Near infrared band	Blue band
False color synthetic band	Red band	Green band	Blue band

In Figure 6 the false color synthesis images are shown in Table 1. From the images, it is clear that highways, buildings and other objects can be distinguished. The distinction between these objects and the background in the transformed images is much greater than that of the original images.

In order to separate more effectively the shadow from the artificial ground objects, the false color images of context are converted from RGB to HSI space. In HSI space, letters H, S and I are respectively referred to the hue, the saturation, and the brightness, which correspond to three basic characteristics that human use to distinguish different colors. HSI space has the unique characteristics in processing image: Since HSI corresponds to three basic features, application of HIS space strategy can avoid the problems that components like luminance and chroma are not independent and each component do not



FIGURE 6. The false color synthetic images

accord with human visual perception. Moreover, these features make HIS space obviously suitable for the image algorithms, which aim to process human visual perception based color perception[16-19]. These features make the HSI space very suitable for the image algorithm, which, based on the visual system of human, is used to process the color perception characteristics[8]. Next, we give the transformation equations of RGB space converted into HSI. The transformation equation of hue is as follows:

$$H = \begin{cases} \theta & B \leq G \\ 360 - \theta & B > G \end{cases} \quad (4)$$

$$\theta = \arccos \left\{ \frac{\frac{1}{2}[(R-G)+(R-B)]}{[(R-G)^2+(R-B)(G-B)]^{\frac{1}{2}}} \right\} \quad (5)$$

The transformation equation of saturation is given as follows:

$$S = 1 - \frac{3}{(R+G+B)} [\min(R, G, B)] \quad (6)$$

The transformation equation of luminance can be calculated by the following formula:

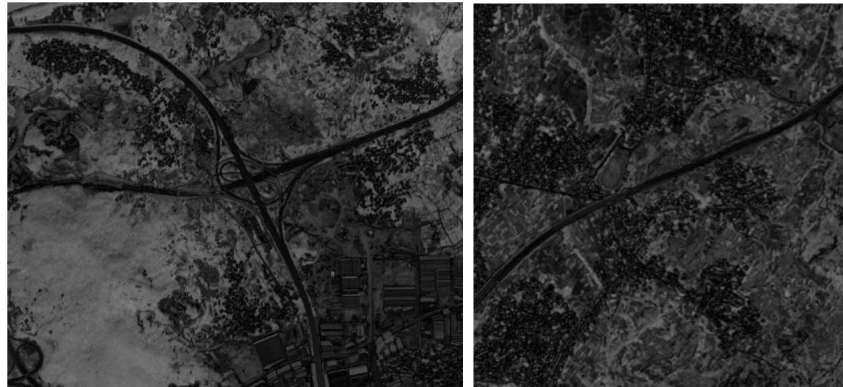
$$I = \frac{1}{3} (R + G + B) \quad (7)$$

The images of Figure 6 converted from RGB space to HSI space are shown in Figure 7.

As can be seen from Figure 7, the artificial ground objects and the relevant shadows cannot be distinguished in the H component of images. In the S component of images, the artificial ground objects and the relevant shadows are different in gray level and the highway in the artificial ground objects is shown as a whole of uniform gray in the images. In the I component of images, the relevant shadows can also be separated from the highway, but the texture of the highway is broken, and the image is easy to be over-segmented instead of forming a whole. Thus, the S component of images is more suitable to distinguish the artificial ground objects from the relevant shadows. Based on the data of experiment and analysis, in the S component image, with the watershed algorithm, setting the segmentation threshold of artificial ground objects and shadow as 0.1 will lead to the better separation of the shadow from the main body of the artificial ground objects and avoid the over-segmentation. In Figure 8, the artificial ground objects mask images of removing shadow are shown. As can be seen in these images, the shadow of the mask



(a) H component images



(b) S component images



(c) I component images

FIGURE 7. HSI space images

images has been effectively removed and the basic integrity of the artificial ground objects is retained.

**3.3. Extracting road by mathematical morphology.** As shown in the Figure 8, although the main body of highway in the mask images is very apparent, there are a large number of building blocks around the highway and many noisy pixels on it. Thus, in the next, the mathematical morphology is further used to remove the building blocks and noisy pixels on the road.

Mathematical morphology is a nonlinear theory based on the set theory, which uses basic logic operations of set to describe and implement the complex image processing algorithms [9,20,21], and it may be treated as an approach to extract the image component. Two

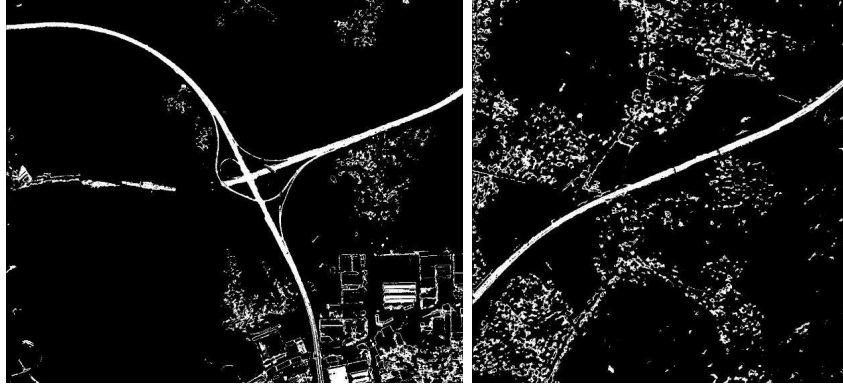


FIGURE 8. Artificial ground objects mask images after removing the shadow

basic operations of mathematical morphology are expansion and erosion, respectively. Suppose symbols  $A$  and  $B$  respectively represent the original image and calculated image, and mark expansion operation with symbol  $\oplus$ , and  $A \oplus B$ , which refers to  $A$  is expanded by  $B$ , is defined as following formula:

$$A \oplus B = \left\{ x \mid \left[ \left( \hat{B} \right)_x \cap A \right] \neq \emptyset \right\} \quad (8)$$

Mark erosion operation with the symbol  $\ominus$ , and  $A \ominus B$ , which refers to  $A$  is corroded by  $B$ , can be defined as follows:

$$A \ominus B = \{ X \mid (B)_x \subseteq A \} \quad (9)$$

The operations of expansion and erosion may be used in cascade mode, i.e. the image is firstly expanded and then corroded, which is so-called open. Mark open operation with the symbol  $\circ$ , and  $A \circ B$ , i.e.  $A$  is opened by  $B$ , is defined as following:

$$A \circ B = (A \ominus B) \oplus B \quad (10)$$

Moreover, the operation on the image in such cascade mode as corroding followed by expanding is called close, which is marked with  $\bullet$ . Expression  $A \bullet B$ , which is referred to as  $A$  is closed by  $B$ , can be defined as follows:

$$A \bullet B = (A \oplus B) \ominus B \quad (11)$$

**3.3.1. Removing non-highway blocks.** Since in general, the highway in the images is in the form of the long and linear shapes, which are apparently different from the rectangular shape of the factory and the building and the irregular shape of the low housing group, the morphological reconstruction operation of the mathematical morphology is suitable to remove the non-highway block. Morphological reconstruction operation works in the following two steps: first, a labeled image is acquired from the original image that is corroded by a specific shape of the structural element according to the geometrical features of the objects; then, in order to acquire the desired image of the objects, the original images are used as the mask images and recalculated with the labeled image[9]. In this work, considering the characteristics of the linear structure of the highway, firstly, the long linear structure element is selected to perform the open operation on the three images of Figure 8, and then an erosion operation on the result of the previous step is performed to gain the labeled image. After that, the results of the opening operation are used as



mask images to reconstruct the network structure of highway. In Figure 9, which gives the results of the morphological reconstruction operation, it is obvious that all the blocks besides the highway have been removed. But there are also obvious defects in the network structure, such as holes, burr, etc., which needs further processing.

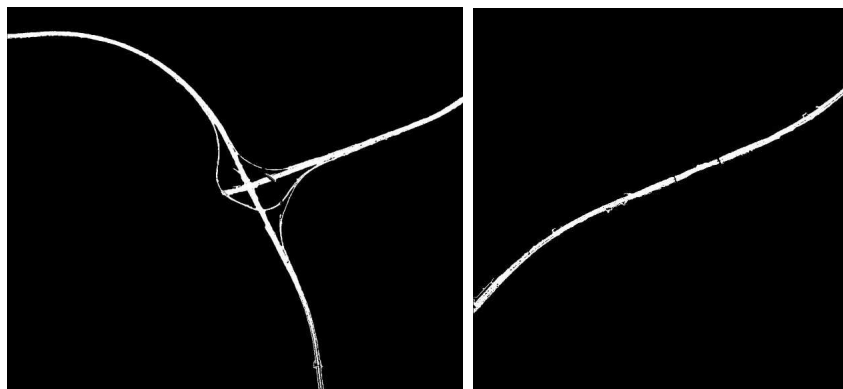


FIGURE 9. Extraction of network structure of highway

3.3.2. *Elimination of voids and burr.* Close operation on the highway network in Figure 9 is performed by using the circular structure element. As a result, the narrow gaps in the images are connected, the holes smaller than structure element are filled and the contour of objects is smoothed. The highway network after close operation is shown in Figure 10, and it can be seen that the hole and burr in the original image have been eliminated significantly, which can be used to extract the highway centerline.

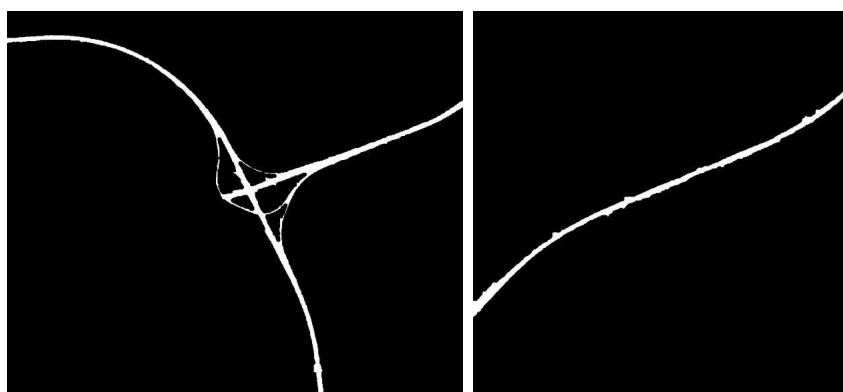


FIGURE 10. Highway network after elimination of voids and burr

3.3.3. *Extracting road centerline.* Nowadays, the technologies of extracting the highway centerline have been very sophisticated and well-developed. Jiang Zhong-Liang et al., for instance, indicate that the mathematical morphology may be used to extract the road centerline[10]; Yang Wei et al. argue that the iterative Meanshift algorithm and segmented Hough transform can be used to extract the road centerline[11]; Tang Rui-hua propose that the algorithms based on the adaptive structure element and the Hilditch refinement can also used to extract road centerline[12]. The commercial software, such as ArcGIS, also has the function to extract the road centerline, which is out of the scope of this paper. In this paper, we directly utilize the centerline extracting function of ArcGIS to obtain the roads centerline. The extracted centerlines from the highway network are

shown in Figure 10, and after extracting the centerline, we overlying the highway network on the original image. By combining the centerlines, the modified version of the original images is shown in Figure 11.



FIGURE 11. Highway centerline extraction

3.3.4. *The result of smoothing.* As seen in Figure 11, the extracted highway center line of the road is basically consistent with the road of remote sensing images, but the extracted center line of the road is not smooth and there are a lot of bumps, seriously affect the smoothness of the road, therefore the center line cannot be used as a result now. Thus, further smoothing is needed to obtain the final result, we use quadratic Bezier curve for smoothing, calculated as follows:

$$P(t) = (P_0 - 2P_1 + P_2)t^2 + (-2P_0 + 2P_1)t + P_0 \quad (12)$$

Wherein,  $P_0, P_1, P_2$  are known points,  $t$  is the smoothing parameter. Road centerline smoothed as shown in Fig12. The obtained results, except for a small part of the road needs human intervention for local modifications, can generally meet the Census highway extraction requirements, and so the automatic extraction for highway is accomplished.



FIGURE 12. Highway centerline after smoothing

3.4. **Comparison with Canny operator.** Figure 13 contains the road centerline extracted by use of Canny operator, you can see from the picture, the road centerline extracted by use of Canny operator presented in the form of short line segment basically, a large number of the centerline of the highway is not extracted, while many places of

non-highway emerge extractions by mistake of the centerline. The reason is that although there are better edge response by use of Canny operator, but the highway cannot be distinguished from the background, so when road centerline is extracted extracting is prone to miss in which difficult to distinguish features and road. While in the linear culture of non-highway extracting is prone to error. As used herein, the method is to make full use of spectral information of remote sensing image, the target road and background make a distinction, and it is possible to minimize the interference of background, when extracting the road can get a more complete road centerline, greatly reducing the missing and error of extracting.



FIGURE 13. Using Canny operator to extract road centerline

**4. Road extraction effect evaluation.** In this paper, we use road location evaluation index to evaluate the road center line extraction effect of highway automatic extraction technology, and compare it with the Canny operators road center line extraction effect[22]. Road location evaluation indices including integrity, correctness, road location mean square deviation and other indices, by calculating the above indices can reflect the quality of road extraction. The indices are defined as follows.

$$Integrity = \frac{\text{Correctly matched reference road length}}{\text{Reference road length}} \quad (13)$$

$$Correctness = \frac{\text{Correctly matching extracted road length}}{\text{Extraction of road length}} \quad (14)$$

Road location mean square deviation

$$= \sqrt{\frac{\sum_1^n (\text{Correctly matching the road location} - \text{Refer to the road location})^2}{2n}} \quad (15)$$

In Figure 14, the center line of the road which is extracted from the artificial image is used as the reference road of the road location evaluation index. The center line of the road is regarded as the axis and a certain width is the tolerance range. While the evaluated road center line is within this range, that the reference road and the evaluation road are considered to be matched.

The results of road center line extracted using the method proposed in this paper are compared with Canny operator, as shown in Table 5. It can be seen from the table that the method proposed in this article is better than Canny operator in terms of integrity,



FIGURE 14. Reference road

correctness and Road location mean square deviation. It is shown that the road center line more complete than Canny operator, and the extraction precision is also slightly better than Canny operator.

TABLE 2. Comparison of road location evaluation indexes

	The method proposed in this article		Canny operator	
	Fig1	Fig2	Fig1	Fig2
Integrity	0.95	0.96	0.27	0.36
Correctness	0.91	0.92	0.58	0.41
Location mean square deviation	0.43	0.33	0.61	0.56

**5. Conclusions.** Based on the characteristic analysis of the image data sources, we propose a technology for the automatic extraction of highway, which is derived from the spectral information of remote sensing images and the mathematical morphology. The extracting images generated by the proposal meet the requirements of highway extraction. However, there are still some defects in our approach, e.g. when applying to the more complex highway, the images of the automatic extraction do not include all of the roads, which could be the direction of the future work.

## REFERENCES

- [1] R. Xu, A Multistage Method for Road Extraction from Optical Remotely Sensed Imagery, *Journal of Information Hiding and Multimedia Signal Processing*, vol.7, no.2, pp.438-447, 2016.
- [2] H. Li, Road extraction and modeling with LiDAR and RS image in urban area, *Acta Geodaetica Et Cartographica Sinica*, vol.40, no.1, pp.133-133, 2011.
- [3] A. F. Zhou, J. X. Zhou, A methodology for road extraction from high resolution remote sensing images, *Remote Sensing Technology and Application*, vol.27, no.1, pp.94-99, 2012.
- [4] L. Y. Zhang, Y. S. Shao, Y. Yang, and Y. Han, Road extraction from high resolution remote sensing images based on the improved mean shift algorithm method, *Remote Sensing Information*, vol.32, no.4, pp.3-7, 2010.
- [5] C. Chen, Q. Qin, N. Zhang (eds.), Extraction of bridges over water from high-resolution optical remote-sensing images based on mathematical morphology, *International Journal of Remote Sensing*, vol.35, no.10, pp.3664-3682, 2014.
- [6] Q. X. Tong, B. Zhang, L. F. Zheng, *Hyperspectral Remote Sensing: Pricipal, Technology and Application*, Beijing, China, 2006.

- [7] H. Zhu, H. Sun, A secondary framework for small targets segmentation In Remote Sensing Images, *Intelligent Computing and Internet of Things (ICIT), 2014 International Conference on. IEEE*, 2015.
- [8] H. Zhao, Y. Jiang, T. Wang (eds.), A method based on the adaptive cuckoo search algorithm for endmember extraction from hyperspectral remote sensing images, *Remote Sensing Letters*, vol.7, no.3, pp.289–297, 2016.
- [9] L. W. LI, J. P. Yin, Road extraction from high resolution remote sensing image based on mathematic morphology, *Remote Sensing Information*, pp.9–9, 2005.
- [10] Z. L. Jiang, M. H. Yang, D. D Yang, The centerline rapid extraction of urban road, *Geomatics and Spatial Information Technology*, vol.38, no.1, pp.3–7, 2015.
- [11] W. Yang, Y. C. Wang, P. P. He, Urban road centerline extraction technology based on LiDAR data, *Geospatial Information*, vol.13, no.4, pp.75–77, 2015.
- [12] R. H. Tang, The automatic road centerline extraction based on adaptive image segmentation, *Engineering of Surveying and Mapping*, vol.24, no.7, pp.29–33, 2015.
- [13] S. U. Yang, T. Shen , A new method for highway extraction in high-resolution SAR image, *Remote Sensing Information*, 2012.
- [14] X. T. Niu, *Highway extraction from high resolution aerial photography using a geometric active contour model*, Ph.D. Thesis, The Ohio State University, 2004.
- [15] S. M. M. Kahaki, M. J. Nordin, Highway traffic incident detection using high-resolution aerial remote sensing imagery, *Science publications*, vol.7, no.6, pp.949–953, 2011.
- [16] Z. Sun, H. Fang, M. Deng (eds.), Regular Shape Similarity Index: A novel index for accurate extraction of regular objects from remote sensing images, *IEEE Transactions on Geoscience and Remote Sensing*, vol.53, no.7, pp.3737–3748, 2015.
- [17] B. Sharma, V. K. Katiyar, A. K. Gupta (eds.), The automated vehicle detection of highway traffic images by differential morphological profile, *Journal of Transportation Technologies*, vol.4, no.2, pp.150–156, 2014.
- [18] M. Jalayer, J. Gong, H. Zhou (eds.), Evaluation of Remote-Sensing Technologies for Collecting Roadside Feature Data to Support Highway Safety Manual Implementation, *Transportation Research Board 92nd Annual Meeting*, pp.345–357, 2013.
- [19] H. Y. Li, H. Q. Wang, C. B. Ding, A new solution of automatic building extraction in remote sensing images, *Geoscience and Remote Sensing Symposium, 2006. IGARSS 2006. IEEE International Conference on. IEEE*, pp.3790–3793, 2006.
- [20] X. Hu, V. Tao, Automatic extraction of main road centerlines from high resolution satellite imagery using hierarchical grouping, *Photogrammetric Engineering and Remote Sensing*, vol.73, no.9, pp.1049–1056, 2007.
- [21] L. Wu, Y. A. HU, A survey of automatic road extraction from remote sensing images, *ACTA AUTOMATICA SINICA*, vol.36, no.7, pp.912–922, 2010.